Chinese Science Bulletin 2005 Vol. 50 No. 18 1991—1994

Charge carrier photogeneration in conjugated polymer PhPPV/R6G composite system

WANG Huan & TIAN Wenjing

Key Laboratory for Supramolecular Structure and Materials of Ministry of Education, Jilin University, Changchun 130023, China
Correspondence should be addressed to Tian Wenjing (email: wjtian@jlu.edu.cn)

Abstract **The spectral and polarity dependence of the quantum yield of charge carrier photo-generation was studied by steady-state photocurrent measurement in a single layer PhPPV film, double layer film of PhPPV and R6G and doped film of PhPPV with R6G. The intrinsic and extrinsic charge carrier photogeneration was observed. The result indicates that the quantum efficiency of the double layer device is higher than that of single layer device under reverse bias, but it is opposite under forward bias. The yield of charge carrier photogeneration of the doped film is higher than that of the other two films at both forward and reverse bias because of the increased interface area between the electron donor and acceptor.**

Keywords: conjugated polymer, photoconduction, charge carrier photogeneration, quantum efficiency.

DOI: 10.1360/982005-118

Photoconducting organic materials including conjugated polymers[1−3], organic molecules[4,5], stacked discostic liquid crystals[6,7] and self-assembling organic semiconductors[8,9] have attracted intense interests due to their extraordinary performances. Their charge carrier photogeneration mechanism has been one of the most important subjects of large amounts of publications in view of possible applications in electronic devices such as photovoltaic cells[10−19]. The charge carrier photogeneration together with the separation and collection of the generated electron-hole pairs (excitons) are the vital factors affecting the performance of a photovoltaic cell. Im et al.[10,11] studied the photoconduction in organic donor-acceptor systems with different acceptor concentrations and concluded that at moderate concentration the yield of the photogeneration was virtually invariant regardless of the system because practically every primary excitation was dissociated at a donor-acceptor site, the subsequent escape from the coulombic potential is virtually system-independent and at dopant concentrations >10% the yield of that escape process increases by two to three orders of magnitude. In order to understand the process of the charge carrier photogeneration in a conjugated copolymer phenyl-substituted poly-phenylenevinylene (PhPPV, manufactured by Covion GmbH, Germany) and rhodamine 6G (R6G, purchased from Aldrich) composite system, the spectral and polarity dependence of photoconductivity in a single-layer film of PhPPV, double-layer film of PhPPV and R6G and PhPPV doped with R6G film were studied by steady-state photocurrent measurement.

1 Experimental

Single-layer device was fabricated by spin coating the chloroform solution of PhPPV with a concentration of 0.5% (w%) on ITO coated glass substrate. The thickness of the homogenous films was about 80—180 nm as measured by a Dektak surface profileometer. Al top electrode of 7 mm^2 was evaporated on the polymer films. Double-layer device was prepared by evaporating a thin layer (about 20 nm) R6G on the polymer films before the evaporation of Al. The position of the highest occupied molecular orbital (HOMO) and the lowest unoccupied molecular orbital (LUMO) of PhPPV and R6G were measured by cyclic voltammetry experiment. UV-Vis absorption spectra of the films were measured with a Perkin-Elmer, Lamda 9 UV/VIS/NIR spectrophotometer.

Photocurrent measurements were performed in a vacuum chamber with a combination of monochromator and a xenon lamp as a light source. Photocurrent signals were detected with a lock-in amplifier (Stanford Research System, Model SR850 DSP), which was connected to a chopper operating at a frequency of 20 to 40 Hz. The benefit of employing the lock-in technique is that it automatically subtracts the dark current from the measured signals. In the course of the routine measurements samples were shortened and kept in the dark for at least several minutes after dozens of measurements. All measurements were finished at room temperature. To calculate the electrical field in ITO/PhPPV/Al diodes a built-in potential of 0.6 eV between Al and ITO electrodes has been taken into account.

2 Results and discussion

The definition of charge carrier photogeneration quantum yield is a fraction of generated charge carrier number (N_{ch}) per absorbed photon number ($N_{\text{abs.ph}}$),

$$\varphi_{\text{ph}}=\frac{N_{\text{ch}}}{N_{\text{abs.ph}}}. \tag{1}$$

In the praxis, a generated charge carrier number can be calculated from a measured photocurrent, $I_{\text{ph}}=N_{\text{ch}}\cdot e$, while an absorbed photon number is calculated from a lamp performance P_{lamp} and a fraction of active material absorption n_{abs}:

$$N_{\text{abs.ph}}=n(\text{all photons from a lamp})\cdot n_{\text{abs}}=\frac{P_{\text{lamp}}}{h\nu}\cdot n_{\text{abs}}. \tag{2}$$

As a result, one can obtain the following equation to calculate a quantum yield for a common steady state photoconduction measurement:

$$\varphi_{\mathrm{ph}}=\frac{I_{\mathrm{ph}}}{P_{\mathrm{lamp}}\cdot N_{\mathrm{abs.ph}}\cdot e}=\frac{I_{\mathrm{ph}}\cdot h\nu}{P_{\mathrm{lamp}}\cdot n_{\mathrm{abs}}\cdot e}. \qquad (3)$$

In order to calculate the exact quantum yield, one should decide whether the generation type is intrinsic volume ionization in the full active area or extrinsic surface sensitized to charge carrier photogeneration. If the type of charge carrier photogeneration is assumed to be an intrinsic case, the quantum yield can be calculated by dividing the number of generated electrons by the full number of absorbed photons in the active film. But if the charge carrier photogeneration is mainly an ITO surface-sensitized case, the electrode-sensitized current has to be normalized to the number of the photons absorbed within a thin layer of thickness l_d from the ITO/film interface, i.e. to $I_0\cdot\alpha\cdot l_d$ where I_0 is the intensity at the interface and $\alpha = 2.3\ \mathrm{OD}/L$ is the penetration and OD is the optical density of a film of thickness L.

Here we have to mention that IPCE (incident photon to current efficiency) is generally accepted to evaluate the performance of photovoltaic system[20−22], which is calculated as follows:

$$\mathrm{IPCE}=\frac{N_{\mathrm{ch}}}{n}=\frac{1240*I_{\mathrm{sc}}}{\lambda*P_{\mathrm{in}}}=\frac{h\nu*I_{\mathrm{sc}}}{P_{\mathrm{in}}*e}, \qquad (4)$$

where I_{sc} is the photocurrent of the device, which is the same as I_{ph} in eq. (3), P_{in} is the incident power, i.e. lamp performance, P_{lamp}. By comparing eq. (3) with eq. (4), it is found that the difference between the charge carrier photogeneration quantum yield used in this paper and IPCE is that in IPCE only lamp performance was considered, while in eq. (3) apart from the lamp performance, the absorbed photons by the active material are calculated. Actually, only the absorbed photons can take part in the charg carrier photogeneration. Apparently the charge carrier photogeneration quantum yield expressed by eq. (3) is more precise for studying the process of charge carrier photogeneration.

Figs. 1 and 2 show the molecular structures of PhPPV and R6G, the UV-Vis absorption of the single-layer PhPPV film, R6G film and double-layer PhPPV-R6G film on quartz substrate. They show that the absorption spectrum of the double-layer PhPPV-R6G film is a simple superposition of the two components, which indicates that there is no interaction between the two materials in the ground state. The energy levels of PhPPV and R6G are shown in Fig. 3. Because both the HOMO and LUMO levels of R6G are lower than those of PhPPV, the charge transfer between the two materials would be expected.

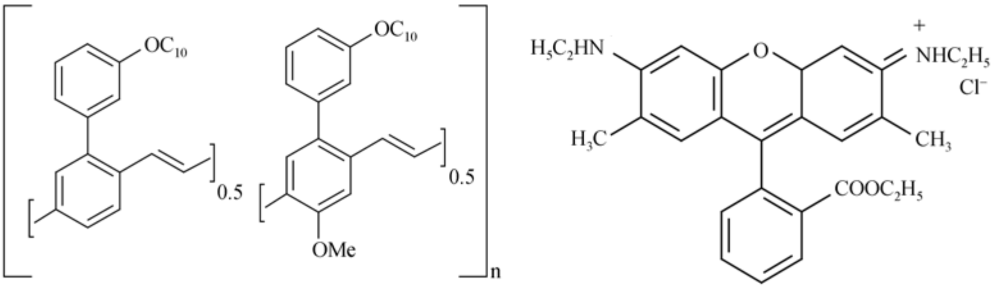

PhPPV R6G

Fig. 1. Molecular structure of PhPPV and R6G.

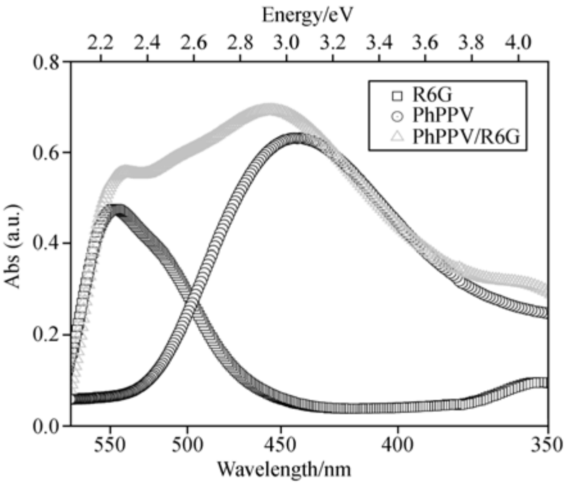

Fig. 2. Solid-state absorption of PhPPV and R6G.

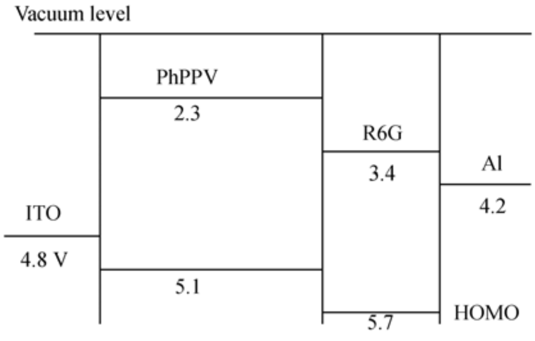

Fig. 3. Diagram of the energy levels of PhPPV and R6G.

The quantum efficiency η of device ITO/PhPPV/Al as a function of the excitation wavelength is shown in Fig. 4.

In Fig. 4 the empty circle refers to the quantum (η_+) when illuminating through the ITO electrode at forward

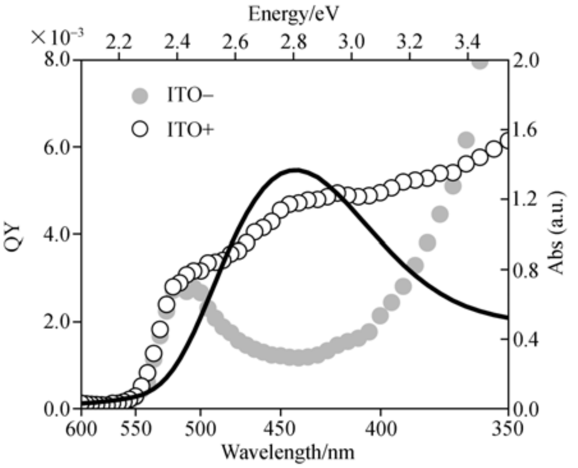

Fig. 4. Charge carrier photogeneration quantum yield (η) of device ITO/PhPPV/Al under forward bias (ITO+) and reverse bias (ITO–) with the electric field of 1×10^5 V/cm.

(positive) bias, and the solid circle pertains to the quantum efficiency (η_-) under reverse bias. Qualitatively, the photocurrent under forward bias is sympatric with the absorption. While the quantum efficiency η_+ is more or less constant within the entire absorption range. But under reverse bias, the quantum efficiency η_- differs from η_+, that is, there is a valley minimum consistent with the maximum of the film absorption, and the ratio of η_+/η_- is about 5 across this shallow minimum.

These experimental results could be virtually interpreted as below. There are three types of mechanisms that photoexcited charge carriers could be generated in a π-conjugated polymer sandwiched between two electrodes: (ⅰ) Excited molecules near the illuminated electrode are photosensitized; (ⅱ) in materials with dopant or inadvertent impurities, trapping energy level under the first excited state can occur; (ⅲ) electrons excited by photons in ground state directly become charge carriers, which is usually defined as an intrinsic photogeneration that commences at relatively high photon energy.

Within a spectral range covering the S_1-S_0 transition, the photosensitized and dopant-sensitized mechanisms are virtually competitive and operate. When the illuminated ITO electrode is positive, i.e. under forward bias, it favors photogenerated charge carrier whose holes are injected into PhPPV layer, while PhPPV chains contiguous to the ITO surface are excited simultaneously. However, under reverse bias, electrons injected into PhPPV layer from the illuminated electrode ITO will combine with holes generated in the excited PhPPV. The bias dependence of the photoresponse in PhPPV confirms this notion.

In the long wavelength part of the absorption spectra, the difference between η_+ and η_- diminishes because photons were less absorbed and then dopant-sensitized process dominated. And at the high energy absorption initial stages, intrinsic photogeneration is suitable, which makes η_- increase steeply.

Under reverse bias and strong absorption, η_- can be expressed by the equation below[11]:

$$\eta_- = \eta_{\mathrm{CT}} \cdot \eta_{\mathrm{esc}} \cdot (2.3\ \mathrm{OD})^{-1},$$

in which η_{CT} is the probability that the excited states create a geminately bound electron-hole pairs; η_{esc} is the yield for subsequent escape from the coulombic potential; OD is optical density. From the equation we conclude that η_- has a minimum at the maximum of the absorption wavelength and increases dramatically at high energy absorption range.

Fig. 5 is the charge carrier photogeneration quantum yield of single layer device ITO/PhPPV/Al and double layer device ITO/PhPPV/R6G/Al under forward and reverse bias. It is shown that the quantum efficiency of the double layer device is lower than that of single layer device under forward bias, but it is opposite under reverse bias. It is because under forward bias holes must be got across the energy barrier formed by the high-occupied molecular orbit (HOMO) of PhPPV and R6G to get to the Al electrode in the bi-layer device, but in single layer de-

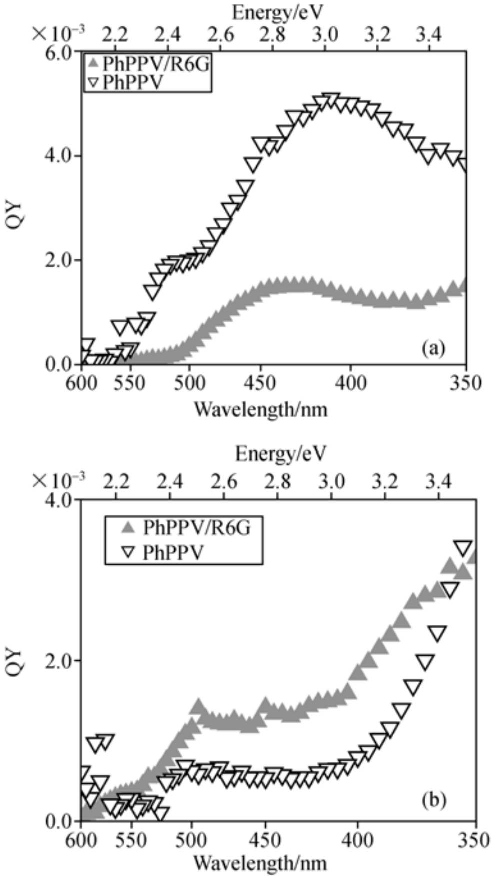

Fig. 5. Charge carrier photogeneration quantum yield (η) of device ITO/PhPPV/Al and ITO/PhPPV/R6G/Al under (a) forward bias (ITO+) and (b) reverse bias (ITO–) with the electric field of 1×10^5 V/cm.

vice this process is precluded. While under reverse bias, holes need not overcome the energy barrier either in the single layer device or in the bi-layer device. Thus, with the electron acceptor R6G, the bi-layer device has much higher quantum efficiency.

Fig. 6 shows the charge carrier photogeneration quantum yield of device ITO/PhPPV:R6G (80:20)/Al under forward and reverse bias. The yield of charge carrier photogeneration of this doped device is approximately 0.01 which is higher than that of bi-layer device under both forward and reverse bias. In doped system, the interface area between electron donor and acceptor is so greatly enlarged that charge separation and transfer are more efficient. Although the efficiency of the photovoltaic device is relatively low compared to the actual application, it will be improved greatly by optimizing the device structure.

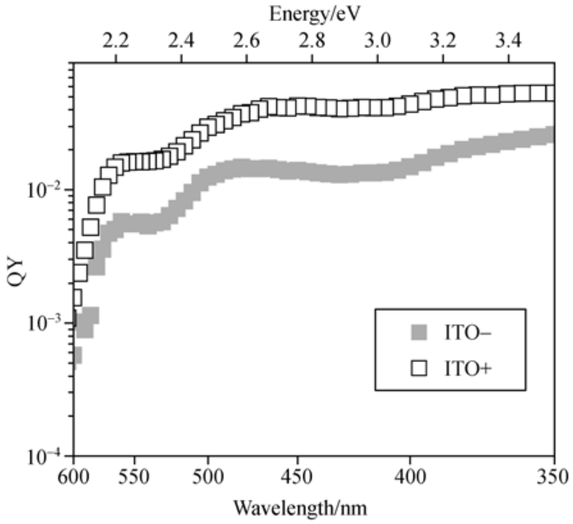

Fig. 6. Charge carrier photogeneration quantum yield (η) of device ITO/PhPPV:R6G(80:20)/Al under (a) forward bias (ITO+) and (b) reverse bias (ITO−) with the electric field of 1×10^5 V/cm.

In conclusion, the intrinsic and extrinsic carrier photogeneration was observed by means of steady state photocurrent investigation of single layer, double layer and doped device and the mechanism of the photogeneration was discussed. For the device ITO/PhPPV/Al, it is indicated that in the long wavelength part of the absorption spectra dopant-sensitized process dominated, while in the middle wavelength the photosensitized and dopant-sensitized mechanisms are virtually competitive and operate simultaneously, and at the high energy absorption initial stages intrinsic photogeneration is suitable. For the device ITO/PhPPV/R6G/Al, polarity dependence of the quantum yield of charge carrier photogeneration is due to the barrier between the LUMO of the donor and the accepter.

Acknowledgements The authors are grateful to Prof. Heinz Bässler and Dr. Im Chan in Philipps-University, Marburg, Germany for their kind help and discussion. This work was supported by the Major State Basic Research Development Program (Grant No. 2002CB613401), the National Natural Science Foundation of China (Grant No. 20474023) and the Program for Changjiang Scholars and Innovative Research Team in University.

References

1. Halls, J. J. M., Walsh, C. A., Greenham, N. C. et al., Efficient photodiodes from interpenetrating polymer networks, Nature, 1995, 376: 498—500.[DOI]
2. Yu, G., Gao, J., Hummelen, J. C. et al., Polymer photovoltaic cells: enhanced efficiencies via a network of internal donor-accepter heterojunctions, Science, 1995, 270: 1789—1791.
3. Camaioni, N., Ridolfi, G., Casalbore-Miceli, G. et al., The effect of a mild thermal treatment on the performance of poly(3-alkylthiophene)/fullerene solar cells, Adv. Mater., 2002, 14(23): 1735—1738. [DOI]
4. Tang, C. W., Two-layer organic photovoltaic cell, Appl. Phys. Lett., 1986, 48(2): 183—185. [DOI]
5. Petritsch, K., Dittmer, J. J., Marseglia, E. A. et al., Dye-based donor/accptor solar cells, Sol. Energy Mater. Sol. Cell, 2000, 61: 63—72. [DOI]
6. Adam, D., Schuhmacher, P., Slmmerer, J. et al., Fast photoconduction in the highly ordered columnar phase of a discotic liquid crystal, Nature, 1994, 371: 141—143. [DOI]
7. Schmidt-Mende, L., Fechtenkötter, A., Müllen, K. et al., Self-organized discotic liquid crystals for high-efficiency organic photovoltaics, Science, 2001, 293: 1119—1122. [DOI]
8. Gregg, B. A., Fox, M. A., Bard, A. J., Photovoltaic effect in symmetrical cells of a liquid crystal porphyrin, J. Phys. Chem., 1990, 94: 1586—1598. [DOI]
9. Liu, C. Y., Pan, H. L., Tang, H. et al., Effect of structural order on the dark current and photocurrent in zinc octakisfl-decoxyethy1 porphyrin thin-layer cells, J. Phys. Chem., 1995, 96: 7632—7636.
10. Im, C., Emeilanova, E. V., Bässler, H., Intrinsic and extrinsic charge carrier photogeneration in phenyl-substituted polyphenylenevinylene-trinitrofluorenone blend systems, J. Chem. Phys., 2002, 117(6): 2961—2967. [DOI]
11. Im, C., Tian, W., Bässler, H., Photoconduction in organic donor-acceptor systems, J. Chem. Phys., 2003, 119(7): 3952—3957. [DOI]
12. Barth, S., Bässler, H., Rost, H. et al., Extrinsic and intrinsic dc photoconductivity in a conjugated polymer, Phys. Rev. B, 1997, 56(7): 3844—3851. [DOI]
13. Arkhipov, V. I., Emelianova, E. V., Bässler, H., Hot exciton dissociation in a conjugated polymer, Phys. Rev. Lett, 1999, 82(6): 1321—1324. [DOI]
14. Pan, J. Y., Scherf, U., Schreiber, A. et al., Xerographic study on a ladder-type poly.para-phenylene., J. Chem. Phys., 2000, 112(9): 4305—4309. [DOI]
15. Arkhipov, V. I., Emeilanova, E. V., Kadashchuk, A. et al., Hopping model of thermally stimulated photoluminescence in disordered organic materials, Chem. Phys., 2001, 266: 97—108. [DOI]
16. Gulbinas, V., Zaushitsyn, Y., Sundstrom, V. et al., Dynamics of the electric field-assisted charge carrier photogeneration in ladder-type poly(para-phenylene) at a low excitation intensity, Phys. Rev. Lett., 2002, 89(10): 107401-1—107401-4.
17. Bässler, H., Arkhipov, V. I., Emeilanova, E. V. et al., Excitons in p-conjugated polymers, Synth. Met., 2003, 135-136: 377—382. [DOI]
18. Lupton, J. M., Im, C. Bässler, H., Fast field-induced dissociation and recombination of optical excitations in a π-conjugated polymer, J. Phys. D: Appl. Phys., 2003, 36: 1171—1175. [DOI]
19. Arkhipov, V. I., Emeilanova, E. V., Bässler, H., On the role of spectral diffusion of excitons in sensitized photoconduction in conjugated polymers, Chem. Phys. Lett., 2004, 383: 166—170. [DOI]
20. Li, J., Sun, N., Guo, Z. et al., Photovoltaic devices with methanofullerenes as electron acceptors, J. Phys. Chem. B, 2002, 106: 11509—11514. [DOI]
21. Deng, X., Zheng, L., Yang, C. et al., Polymer photovoltaic devices fabricated with blends MEHPPV and organic small molecules, J. Phys. Chem. B, 2004, 108: 3451—3456. [DOI]
22. Winder, C., Sariciftci, N. S., Low bandgap polymers for photon harvesting in bulk heterojunction solar cells, J. Mater. Chem., 2004, 14: 1077—1086. [DOI]

(Received January 18, 2005; accepted February 28, 2005)